Journal of Organometallic Chemistry 893 (2019) 85–92

Contents lists available at ScienceDirect

Journal of Organometallic Chemistry

journal homepage: www.elsevier.com/locate/jorganchem

DFT study of carbene formation and olefin metathesis catalyzed by $[RuCl_2(PPh_3)_2(Py)_2]$ complex

Hudson Gomes Evangelista [a, b], José Milton Elias de Matos [a, **], Égil Sá [a, c, *]

[a] Laboratório Interdisciplinar de Materiais Avançados (LIMAV), Centro de Ciências da Natureza, 64049-505, Inninga, Teresina-PI, Brazil
[b] Laboratório Central Analítica de Química/CCET- Universidade Federal do Maranhão-UFMA. Av. dos Portugueses, 1966-Vila Bacanga, 65080-805, São Luís-MA, Brazil
[c] Universidade Federal do Piauí, Campus Ministro Reis Veloso, 64202-020, Parnaíba-PI, Brazil

ARTICLE INFO

Article history:
Received 13 January 2019
Received in revised form
19 April 2019
Accepted 26 April 2019
Available online 30 April 2019

Keywords:
Olefin metathesis
ROMP
DFT calculations
Carbene formation
Mechanism

ABSTRACT

A DFT approach was used to clarify the structure of $[RuCl_2(PPh_3)_2(Py)_2]$ complex, which came out to be hexacoordinate with the similar ligands *trans*-positioned regarding each other. We addressed different pathways analyzing the formation of $[RuCl_2(Py)_2(=CHCOOCH_2CH_3)]$ carbene active species using $[RuCl_2(PPh_3)_2(Py)_2]$ and ethyldiazoacetate. Our findings show that the mechanism most likely to happen presents an immediate coordination of the C_α of the EDA to the ruthenium atom, with an affordable activation energy (10.5 kcal·mol^{-1}). Subsequent ring opening metathesis of norbornene catalyzed by the ruthenium-carbene active species is also considered. Experimental yields available in the literature present correlation with the activation energy and the favorability of the products in our mechanism.

1. Introduction

Olefin metathesis is a reaction that promotes the interchange of alkylidene groups (=CRR') of two different olefins, through breaking and formation of C=C bonds. It is a powerful tool for a variety of usage, especially in organic synthesis and polymer chemistry [1–6]. Regarding the polymer chemistry, Ring Opening Polymerization (ROMP) is useful to polymerize cyclic olefins [7].

The reaction mechanism was proposed in the early 70s by Chauvin and Hérrison [8], and afterward widely proved and accepted, demonstrating that is necessary the existence of an active species metal-carbene (M = CRR'). The processe takes place through the coordination of the incoming first olefin (the cyclo-addition process) followed by the formation of the intermediate metallacyclebutane that immediately suffers the cycloreversion process, forming a new metal-carbene. The second olefin then enters the catalytic cycle and performs the same steps, concluding the metathesis of two different olefins.

The enlightenment of this mechanism showed the fundamental role played by the active species metal-carbene, which paved the way for the development of the so-called well-defined catalysts. There are two main groups of such catalysts, both containing metal-carbene fragment. The first of these groups to appear is composed by complexes of W, Mo, Nb, the so-called Schrock's catalysts. Those catalysts presents an interesting reactivity, being even able to react with electron deficient or substituted olefins [9]. However, some problems appeared in environments of protic solvents, moisture or oxygen, leading to the decomposition of the catalysts [10].

The other class of catalyst are the Grubbs' catalysts [11], which are based in Ru-carbenes, and responsible for the popularization of olefin metathesis, mainly because these ruthenium complexes can react with a bigger number of different olefins substrates, since they are more resistant to acid, protic and oxygen-containing media, although less reactive regarding the Schrock catalysts. They started with complexes known as 1st generation, with $(PCy_3)_2Cl_2Ru=CHPh$ as general formula, which are more stable, although less reactive than Schrock complexes. A significant improvement came in the 2nd generation, replacing a phosphine by a carbene N-heterocyclic – $(H_2IMes)(PCy_3)Cl_2Ru=CHPh$ –

* Corresponding author. adress: Laboratório Interdisciplinar de Materiais Avançados (LIMAV), Centro de Ciências da Natureza, 64049-505, Inninga, Teresina-PI, Brazil.
** Corresponding author. .
E-mail addresses: jmematos@ufpi.edu.br (J.M.E. de Matos), egil.sa@ufpi.edu.br (É. Sá).

https://doi.org/10.1016/j.jorganchem.2019.04.029
0022-328X/

becoming very efficient for metathesis of a diverse number of olefins.

In the ROMP reaction, besides the importance of the metal-carbene, phosphine ligands also play a major role in the initiation process and in the living polymerization itself. In this way, the polymer properties depend on the ligands coordinated to the metallic center, known as ancillary ligands. Although Grubbs complexes are powerful catalysts for Olefin Metathesis, there is a demand for more robust catalyst as a response to the continuous challenge for new materials [6,12].

In the last years, amine ligands have been appearing as important simple and cheap ligands for alternative olefin metathesis catalysts. Similarly to the phosphines, they also can control the electronic density, as well as steric hindrance on the metal coordination sphere towards a high catalytic activity [13]. Within the purpose of providing alternative catalysts for olefin metathesis reaction that bears cheaper and simpler ligands, a series of pre-catalysts has been proposed. Special attention has been paid to develop complexes of the $[RuCl_2(Phosphine)_2(Amine)_y]$ ($y = 1$ or 2) kind, containing both P and N, since they are reasonably non-sensitive to the air, moisture, light and warm, which are some of the appropriated conditions for a large practical application. Such work developed by one of us, together with other colleagues, have shown that a combination of phosphines and amines on the starting non-carbene Ru(II) coordination sphere, catalyses the formation of polymers with interesting results of yield, molecular weights and dispersion [14–24].

There are two families of these complexes above described: one is pentacoordinated [14], with one amine, and the other is hexacoordinated [16], with two amines. The first family is well studied, and the precursor $[RuCl_2(PPh_3)_2(piperidine)]$ well characterized, as having a square base pyramid geometry, with the amine in the apical position and the phosphines in *trans* position regarding each other, as well as the chlorides.

As a matter of fact, these complexes described above are in fact precursors of the active species Ru-carbene, which is generated *in situ* by reacting with ethyl diazoacetate (EDA). The mechanism for the formation of the Ru-carbene and the subsequently ROMP of norbornene is partially proposed, for the case of the pentacoordinated $[RuCl_2(PPh_3)_2(piperidine)]$ complex [25]. After the carbene formation, then the olefin metathesis reaction happens. Alternatively, experimental studies point that the norbornene enters in the catalytic cycle, by coordinating to the ruthenium, before the carbene formation, which clearly plays an important role in the hypothetical mechanism [21]. On the other hand, the structure $[RuCl_2(Phosphine)_2(Amine)_2]$ hexacoordinated complex is not fully characterized and understood, as well as the carbene formation and the subsequent olefin metathesis reaction itself.

In this way, this work is aimed at understanding the structure of the hexacoordinated complex with pyridine being the amine ligand - $[RuCl_2(PPh_3)_2(Py)_2]$. More importantly, we want to explain the mechanism involved in the formation of the Ru-carbene active species and the ring opening metathesis of norbornene.

2. Computational methodology

This work is based on Density Functional Theory. All structures of reactants, products, intermediates and transition states were optimized through B3LYP exchange-correlation functional [26,27]. Main-group atoms were treated with double-zeta plus polarization functions on heavy atoms basis set 6-31G(d) [28,29], except for Ru atoms, to which was used the effective core potential of Hay and Wadt (LanL2DZ) [30–32], henceforward referred as BS1.

All stationary points were characterized by vibrational calculations, where the absence of imaginary frequencies means a minimum geometry, and the presence of only one imaginary frequency implies in a transition state geometry. For the cases whose connectivity between reactants and products was not clear for a given transition state, intrinsic reaction coordinate (IRC) calculations were performed for ensure the reliability of such structure.

To improve the accuracy of the results, single-point calculations were performed on the optimized geometries obtained by means of BSI, with M − 06 [33] exchange-correlation functional while a large basis set, triple-zeta $6–311^{++}G(d,p)$ [28,34], was chosen for all atoms, except ruthenium that was, again, treated with the effective core potential of Hay and Wadt (LanL2DZ). Solvent effects were also included, by means of the Polarizable Continuum Method [35–37], regarding the solvent experimentally used, chloroform ($\varepsilon = 4.7113$). Finally, non-covalent interactions were taken into account employing the Grimme's empirical dispersion (D3) [38]. This level of theory from now on is called BS2. The ΔG energies reported in this text are based on the gas-phase Gibbs correction obtained with BS1, calculated at 298.15 K and 1 atm, added to the energies from BS2. All calculations were performed with Gaussian 09 package [39].

B3LYP has been proved efficient for organometallic studies in general [40–42], including olefin metathesis [43–45]. A comparative study of different GGA, meta-GGA and hybrid-meta-GGA functionals found that B3LYP is generally only slightly less acurate than the newer, dispersion-inclusive functionals, which are more computatinal demanding. They also indicated that single-point calculations on B3LYP optimized structures with M05−2X could be an efficient balance between accuracy and computational cost [46]. As said above, in this work we use a similar methodology, where the structures are optimized with B3LYP followed by single-point calculations with M06, including dispersion and implicit solvation. This level of theory has been successfully used in the organometallic field with complexes of different metals, ruthenium included [47–54].

3. Results and discussion

This work is focused on proposing a mechanism for the ROM of norbornene promoted by the precursor $[RuCl_2(PPh_3)_2(Py)_2]$ complex and EDA, with the *in-situ* generation of the carbene. We explore the mechanism for the formation of the Ru-carbene active species, analyzing three possible paths. Subsequently, ROM of norbornene promoted by the Ru-carbene previously formed, is addressed. Finally, the key steps of the overall proposed mechanism are faced with experimental results. For such a goal, understand the structure of the hexacoordinated precursor is crucial, and we start adressing this issue.

3.1. Structure and activation of the precursor

This complex was synthesized for the first time by Matos and colleagues [16]. In that time, besides the reactivity for the ROMP of norbornene, the authors attested the hexacoordinated nature of the compound with molecular formula $[RuCl_2(PPh^3)_2(Py)_2]$ and a low-spin d^6 electronic configuration. However, the relative positions of the ligands were not clarified. **Fig. 1** shows the possible isomers for the complex, and their relative energy.

It was expected an isomer **a** with ligands *trans*-positioned to be the most stable, since the large PPh_3 groups in a *cis* position would carry out repulsive steric interactions. We found that the isomers **a** and **b** are almost degenerated and, by far - at least 6.0 $kcal \cdot mol^{-1}$ -, the most stables configurations. Isomer **a**, with all ligands in *trans* position regarding each other, is 0.4 $kcal \cdot mol^{-1}$ more stable than isomer **b**. The analysis of the IR spectrum of the five isomers shows the appearance of the stretch bands for the chlorides in *trans*

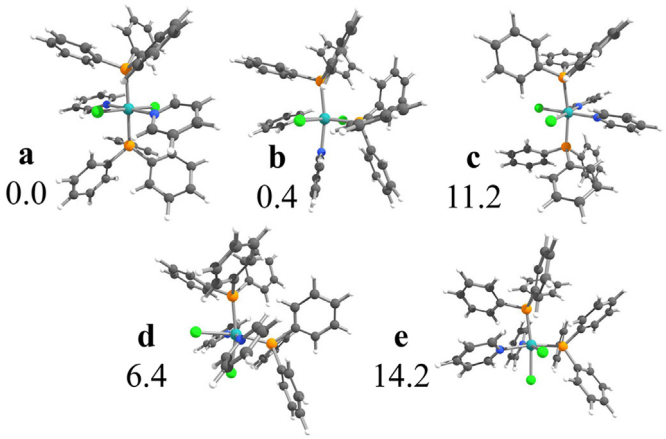

Fig. 1. Potential isomers of the hexacoordinated complex $[RuCl_2(PPh_3)_2(Py)_2]$ and their relative energies, in kcal·mol^{-1}.

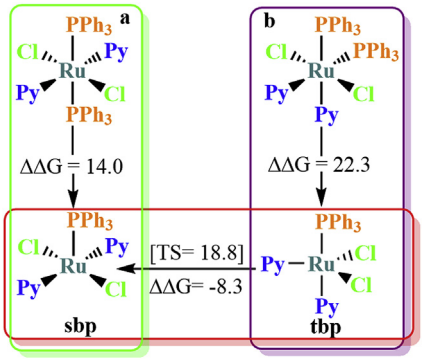

Fig. 2. Activation process to form the **sbp** pentacoordinated active complex. Energies values in kcal·mol^{-1}.

position for the isomers **a** (315 cm^{-1}) and **b** (303 cm^{-1}) (see Figs. S1–S5 in SI), that is within the experimental range register (350-300 cm^{-1}). The isomer **d** also shows a band around 310 cm^{-1}, however, is flatter than the cases **a** and **b**, and is not related with chlorides stretch.

The catalytic precursor is an 18 electrons species, which implies the decoordination of one ligand for any reaction to occur, forming a 16-electron species. There are two possibilities of activation: the loss of one phosphine or the loss of a pyridine. We have considered this both possibilities for complexes **a** and **b**, since they are the most favorable isomers. For all cases, decoordination of ligands is endergonic. Decoordination of a phosphine from **a** ($\Delta G = 14.0$ kcal·mol^{-1}) is less favorable than decoordination of a pyridine group from **b** ($\Delta\Delta G = 4.4$ kcal·mol^{-1}). However, a relaxed scan for these both ligands decoordination, in complexes (**a** and **b**), shows that the phosphine decoordination from **a** is more favorable for than the pyridine decoordination from **b**, by around 5.0 kcal·mol^{-1} (in total energy), and the other cases are even less favorable (see Fig. S6 in SI). Indeed, this corroborates the experimental observations, referring to the appearance of a signal in the NMR spectra for a free phosphine after 2 h, and the absence of a signal for free pyridine [16]. Such behavior is justified, since pyridine is a stronger σ-ligand than phosphine, therefore harder to suffer decoordination.

The processes of the phosphine loss to form the pentacoordinated complex is schematized in **Fig. 2**. When the most stable isomer **a** lose a phosphine, it immediately creates a pentacoordinated complex with a square-base pyramid structure (**sbp**). This is an endergonic process that consumes 14.0 kcal·mol^{-1}. The isomer trigonal bi-pyramid (**tbp**) is 8.3 kcal·mol^{-1}less stable. The isomer hexacoordinated **b**, as said above, is relatively degenerated to the isomer **a**, and can play a relevant role in the reactional environment. Decoordination of a phosphine from **b** implies in the immediate formation of the less stable **tbp** pentacoordinated complex, raising the system energy by 22.3 kcal·mol^{-1}, that only can interconvert in the SBP structure by overcoming a barrier of 18.8 kcal·mol^{-1}. To summarize, in the hexacoordinated complex each pair of similar ligands are in *trans* position (isomer **a**); this complex suffers decoordination of a phosphine to form a square-based pyramid pentacoordinated complex (**sbp**) active species.

3.2. Formation of the Ru-carbene species

After the pentacoordinated **sbp** complex is formed, the carbene catalyst is generated by reacting with EDA, and Chauvin mechanism can therefore operate. Three substances are added in the reactional pot for the overall process: the Ru-complex **a**, EDA and norbornene. In this way, is not clear which reactant, norbornene or EDA, initially interact with the pentacoordinated complex. These two possibilities have been raised as reliable [21], which imply in potential different mechanisms. **Scheme 1** shows the overall mechanisms to be addressed in this work.

Step **A** is the mechanism described in the previous section: the initiation process that occurs by the loss of a phosphine, forming

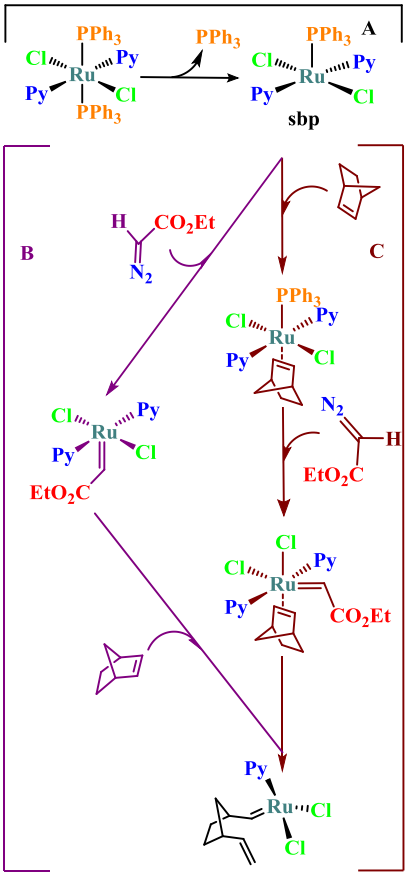

Scheme 1. Potential pathways addressed in this work – A: activation of the precursor; B: formation of the carbene with the pentacoordinated complex and subsequent ROMP; C: formation of the carbene along with the norbornene previously coordinated.

the **sbp** pentacoordinated species, which will be the active species to engage the subsequent steps. The pathway **B** can occur when an EDA molecule coordinates to the **sbp** pentacoordinated complex, to form the carbene. After the carbene formation, an incoming norbornene engages the Chauvin mechanism of ROM. Alternatively, instead of coordination of an EDA molecule to the pentacoordinated complex, we can have initially the coordination of a norbornene, and then formation of carbene with EDA. Therefore, the norbornene, previously coordinate, reacts with the carbene by Chauvin mechanism, performing the ROM. This is shown in pathway **C**. All mechanisms discussed from now on are going to regard the **sbp** pentacoordinated species as the reference.

3.2.1. Pathaway BI – diazo linked

For carbene formation with no previous coordination of NBE (**path C**), there are two possibilities: in the **path BI**, showed in Fig. 3, the diazo fragment of the EDA keeps linked to the ruthenium all along the pathway. In the case of **pathway BII**, henceforward called 'direct attack', the C_α of the carbonyl group of the EDA coordinates directly to the ruthenium center, as shown in Fig. 3. In this same section, we discuss the **pathway BI**. It is similar to another mechanism proposed for the formation of metal-carbenes with diazoalkanes and a Rh–PCP complex [55].

This path starts with the coordination of the EDA to **sbp** complex by one nitrogen (η^1-N) forming the complex **bi.1**, in an endergonic process of 1.3 kcal·mol^{-1}, to subsequently transform in a bihapto coordination (η^2-NN), resulting in the structure **bi.2**, located 9.7 kcal·mol^{-1} above, surpassing a barrier of 10.3 kcal·mol^{-1} (**bi.12$^{\#}$**). By overcoming a barrier of 29.3 kcal·mol^{-1}, the intermediate **bi.3** is formed; such intermediate is a diazirine, formed by the two nitrogen and a carbon atom, coordinated to the **sbp** complex. Subsequently, the diaziridine **bi.3** is transformed in a four-membered ring (**bi.4'**), where two vertices are formed by nitrogens, another by the ruthenium, and the last by the carbon, which is going to form the carbene together with the ruthenium in the end of the catalytic cycle.

The transformation of **bi.3** into **bi.4** shows the largest barrier of this catalytic cycle, 37.1 kcal·mol^{-1}, perhaps because in this step begins the formation of the Ru=C bond. Moreover, in the transformation of **bi.3** to **bi.4'**, occurs a situation where the complex has seven ligands, *ergo* presenting 20 electrons (Ru^{2+} has six valence electrons), although immediately the decoordination of the phosphine takes place, and **bi.4** has again 18 electrons. The Ru–P bond length in the species **bi.3** is 2.46 Å, while in the transition state **bi.34$^{\#}$** is 2.53 Å, indicating the beginning of the phosphine decoordination. The IRC towards the products from this transition state results in a structure where the distance Ru–P is 3.90 Å, which clearly shows that the phosphine is already decoordinated (**bi.4'**). These geometrical parameters can be checked in the Supporting Information.

The following steps cover the path towards decoordination of the N_2 fragment. The trasition state **bi.45$^{\#}$** corresponds to a barrier of 13.0 kcal·mol^{-1}, and is the highest stationary point of this PES. It is associated to the loss of the ruthenium interaction with the nitrogen atom, undoing, therefore, the four-membered ring, resulting in the species **bi.5**. In this stationary point we have the formation of a single bond between the ruthenium and the carbene, to subsequently completely form the Ru=C species **bi.6** by overpassing a barrier of 0.8 kcal·mol^{-1} (**bi.56$^{\#}$**). This step is related with the bond breaking between the N_2 and the carbenic carbon.

Overall, this is a complex pathway with many steps, where **bi.34$^{\#}$** is the most significative barrier (37.1 kcal·mol^{-1}), corresponding to the transformation of the hexacoordinated diazirine **bi.3** into the also hexacoordinated structure **bi.4** with a four-membered ring. The activation energy is 52.1 kcal·mol^{-1}, related to the transition state **bi.45$^{\#}$**. For a given process, such a barrier is very unlike in a productive mechanism.

3.2.2. Pathaway BII – direct attack

This is an alternative mechanism for the formation of the ruthenium-carbene without previous coordination of a norbornene molecule. In here, the EDA bonds to the metallic center of the **sbp** by means of the C_α in the carbonyl group of EDA, instead of the nitrogen, as showed previously. The whole mechanism is pictured in Fig. 4.

First step is the coordination of EDA to the **sbp** pentacoordinated complex, forming an hexacoordinated **bii.1**, by consuming 1.4 kcal·mol^{-1}. The following step is the formation of the pentacoordinated Ru-carbene **bii.2**, overcoming the transition state **bii.12$^{\#}$**, corresponding to a barrier of 9.1 kcal·mol^{-1}. Stationary

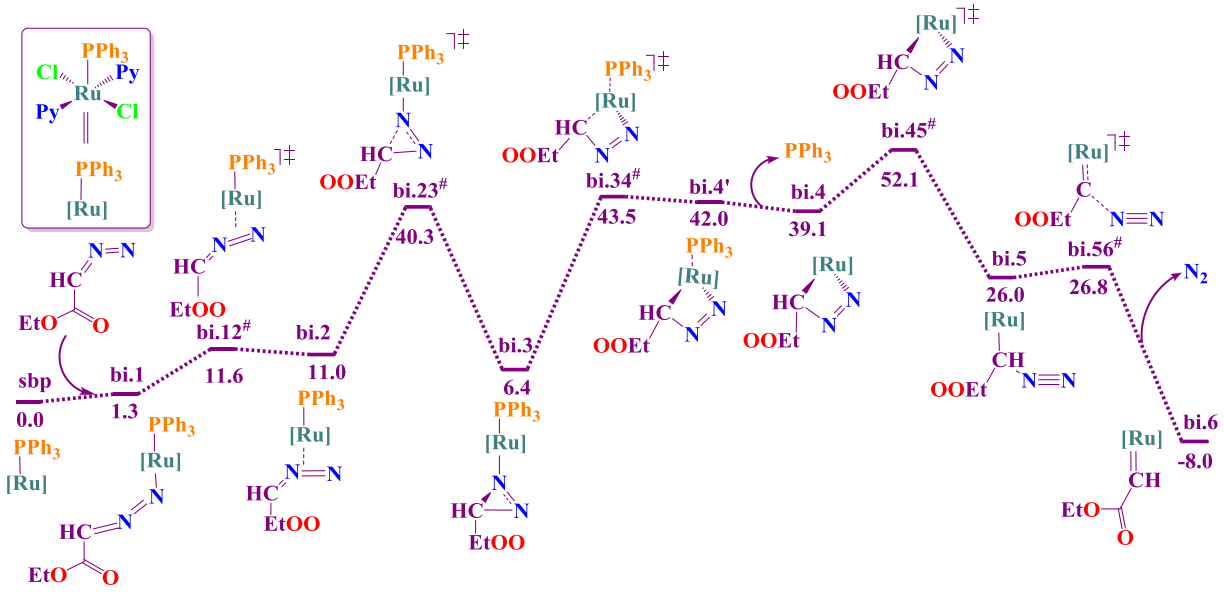

Fig. 3. Mechanism of **pathway BI**–'diazo linked' for the formation of the carbene. Energies in kcal·mol^{-1}.

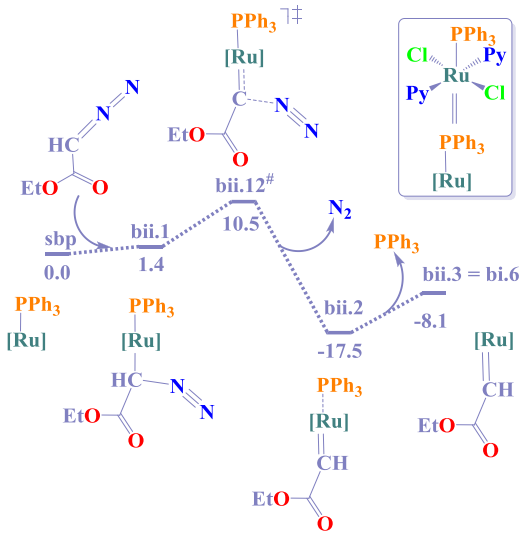

Fig. 4. Mechanism of the **pathway BII**–'direct attack', for the formation of the carbene. Energies in kcal·mol^{-1}.

point **bii.2** is a hexacoordinated structure where the Ru=C bond is already settled, presenting 1.84 Å length, hence within the characteristic boundary for such bond [56–58]. This structure is also considerably exergonic regarding the reactants (−17.5 kcal·mol^{-1}), showing the stability of the ruthenium carbene. In **bii.2**, the bond Ru–P is 3.04 Å length, indicating that the phosphine is already decoordinated. The optimization of the carbene without the phosphine is the pentacoordinated structure **bii.3**, lying 9.4 kcal·mol^{-1} high in energy, resulting in the carbene active species that can catalise ROM of norbornene.

In this pathway, as in previous one, the second phosphine decoordinates spontaneously from the ruthenium center: in **bii.2** the distance Ru–P is 3.04 Å, which is a distance for an uncoordinated ligand. Previously, in the transition state **bii.12#**, this same bond distance is 2.58 Å, which is still a value for a coordinated ligand, and in **bii.1**, the distance Ru–P is 2.34 Å, where the

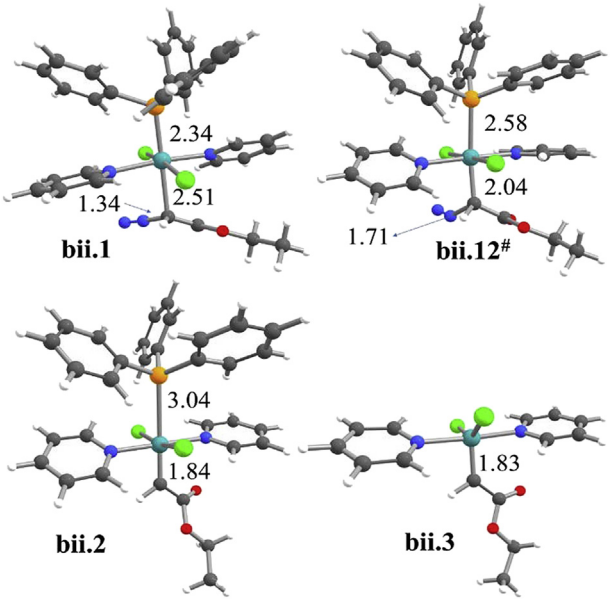

Fig. 5. Geometries of the **pathway BII**–'direct attack'. Bond lengths in Å.

phosphine is effectively coordinated, as can be seen in **Fig. 5**. Perhaps the double bond character of the Ru-carbene (**bii.2**) bond forces the decoordination of the phosphine. This liberation of the second phosphine is corroborated by experimental findings showing that the presence of excess of free phosphines in the solution avoids ROMP. Moreover, the presence of a free phosphine in a *post*-ROMP solution is indicative of a second ligand release [16,19]. This released ligand is not a pyridine, since no evidence of free-pyridine NMR signal was detected [20].

The **pathway BII** is clearly simpler than **pathway BI**, with fewer steps. As a matter of fact, it can be considered as a concerted mechanism, since the formation of the carbene and the releasing of molecular nitrogen (N_2) takes place in a single step, by means of the transition state **bii.12#**, which also engenders the decoordination of the second phosphine. The overall activation energy is 10.5 kcal·mol^{-1} corresponding to the only transition state **bii.12#**, that is 41.6 kcal·mol^{-1} smaller than in the previous mechanism discussed. This indicates that 'direct attack' promotes a mechanism kinetically more reliable than the 'diazo linked'.

3.2.3. *Pathaway C – NBE linked*

This mechanism is different of the two previously discussed, as it is shown in **Fig. 6.** It was suggested in an experimental work [21] about the synthesis of co-polymers with norbornene and norbornadiene, catalyzed by the complex [$RuCl_2(PPh_3)$Pip]. Although this complex has two phosphines and one nitrogenate ligand (piperidine) - and in our case we have one phosphine and one nitrogenate ligands (pyridine) in the **sbp** structure - it is a fair assumption that this mechanism can operate here. Based on the findings discussed in previous sections, we assumed a mechanism based on the **pathway BII** with a direct attack of the carbenic carbon, since it is the preferred mechanism when the NBE is not linked to the ruthenium center.

The starting step is the coordination of a NBE molecule to the

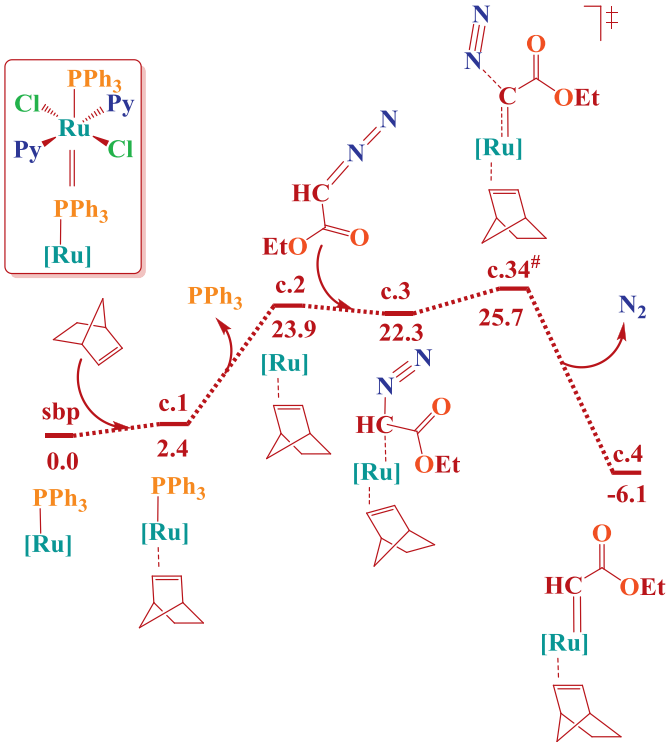

Fig. 6. Mechanism of the **pathway C**–'NBE linked', for the formation of the carbene. Energies in kcal·mol^{-1}.

sbp complex resulting in the species **c.1**. This process occurs by gaining 2.4 kcal·mol^{-1}. The subsequent step would be the coordination of the EDA molecule to the species **c.1**, however all attempts to optimizing a structure with seven ligands failed, and this happens so because this hypothetical complex would have 20 electrons. Therefore, before the coordination of the EDA molecule is necessary one ligand to leave the metallic center. We have found that the phosphine decoordination is 5.6 kcal·mol^{-1} more stable than the pyridine decoordination. In this way, decoordination of the phosphine generates the structure **c.2**, which increases the system energy by 21.5 kcal·mol^{-1}.

An EDA molecule coordinates to the **c.2** species, forming the complex **c.3**, which is a process that lower the energy by 1.6 kcal·mol^{-1}. Now the system overcomes a small barrier (3.4 kcal·mol^{-1}) that corresponds to the transition state **c.34$^{\#}$**. The imaginary frequency of this transition state referes to the elongation of the bond between the carbenic carbon and the nitrogen, and at the same time to the shortening of the distance of the ruthenium to the carbenic carbon, clearly showing the Ru=C bond formation and the releasing of N_2, which is confirmed in the following stationary point, that is the carbene itself (**c.4**). The step from **c.3**→**c.4** is extremely exergonic, lowering 31.8 kcal·mol^{-1} the energy of the system.

In summary, this mechanism is unlike to happen since its activation energy is 25.7 kcal·mol^{-1}, which is 15.2 kcal·mol^{-1} higher than for the case of the mechanism 'direct attack' (see **Fig. 5**). Obviously, coordination of the norbornene molecule carry difficulties to the subsequent steps in this mechanism, since it is necessary the immediate decoordination of one phosphine, that is a step fairly unfavorable (21.5 kcal·mol^{-1}).

After the scrutiny of these three possible mechanisms, we can say that the prevalent mechanism to the formation of the Ruthenium-carbene active species $RuCl_2(Py)_2(=CHCO_2Et)$ is the **pathway BII – 'direct attack'**, without the prior coordination of an NBE molecule.

3.3. ROM of norbornene

In this section we use the carbene **bii.3** (which is the same structure as **bi.6**) to address the Ring Opening Metathesis of norbornene, whose Gibbs energy profile is shown in **Fig. 7**.

In this path, the ruthenium-carbene **r.i** (labeled **bii.3** in the **pathway BII**) is a square-based pyramid pentacoordinated species with two chlorines and two pyridines forming the pyramid's base, and the carbene in the apical position. Subsequently, it loses one of the pyridines, resulting in the species **r.2** that is 15.2 kcal·mol^{-1} higher in energy. The subsequent steps behave similarly to the already well-established mechanisms for olefin metathesis. The incoming olefin, in this case norbornene, coordinates to the ruthenium center releasing 8.6 kcal·mol^{-1}, after which it surpasses the cycloaddition transition step (**r.34$^{\#}$**) to form the intermediate metallacyclebutane **r.4**. The metallacycle easily suffers cycloreversion with a barrier of 2.7 kcal·mol^{-1}, topped by **r.45$^{\#}$** transition state, to finally form the new olefin **r.5**, that is the product of the ROM of the first norbornene molecule. This mechanism is similar to another computational calculations for olefin metathesis with ruthenium-carbenes [43–45].

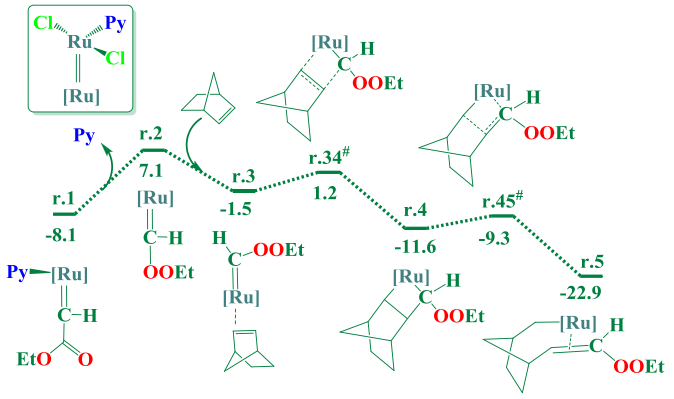

Fig. 7. Mechanism for **ROM** of norbornene catalyzed by $RuCl_2(Py)_2(=CHCO_2Et)$ carbene. Energies in kcal·mol^{-1}. The reference energy (−9.0 kcal·mol^{-1}) corresponds to Ru-carbene product in **pathway BII**.

The complex **r.1** is a 16 electrons species, and without the loss one pyridine would make hard the olefin metathesis reaction. Even so, we have considered it, and the energy profile is shown in Fig. S7 (see in SI). A 16 electrons species could avoid the cycloaddition, since the step corresponding to this process (the analogous to **r.34$^{\#}$**) is a species that could be considered as having 18 electrons, which implies in a more difficult process. Indeed, we have not been able of locate this structure neither the transition state for cycloreversion. Overall potential energy surface should be higher in energy than the one showed in **Fig. 7**. See more in Section S2 in SI.

The complete catalytic cycle for the ROM of norbornene, including the formation of carbene, corresponds to the combination of the pathway BII – direct attack (**Fig. 4**) and the pathway for ROM of norbornene (**Fig. 7**). The activation energy for the whole reaction is 18 kcal·mol^{-1}, that corresponds to the transition state **bii.12$^{\#}$**, which is an affordable barrier, easily compensated by the energy released for the formation of the product **r.5** (−16.7 kcal·mol^{-1}).

As said in the introduction section, to the best of our knowledgement, there is only one computational work about olefin metathesis with this kind of catalyst. In that study, the mechanism for the formation of the Ru-carbene and the subsequently ROM of norbornene is partially proposed for the case of the pentacoordinated $[RuCl_2(PPh_3)_2(piperidine)]$ complex. In our case, after decoordination of one phosphine from the hexacoordinate $[RuCl_2(PPh_3)_2(Py)_2]$, a pentacoordinated complex with only one nitrogenated ligand is formed, as well. For $[RuCl_2(PPh_3)_2(piperidine)]$, the main barrier is the carbene formation, with a value of 12.5 kcal·mol^{-1}, and in our study it is 9.1 kcal·mol^{-1}. On the other hand, the general activation energy for the complex with piperidine is smaller than with pyridine. The studies, however, were not performed in the same level of theory, since the work of Haiduke et al. does not include dispersion correction. Moreover, their work does not assembly a systematic study about the mechanism for the formation of Ru-carbene, instead they focus only on the ROMP of norbornene [25].

3.4. Influence of N^{III} substituent in the reactivity

Experiments have shown that the change of the N^{III} substituent in the hexacoordinated complex $[RuCl_2(PPh_3)_2(Py)_2]$ influences directly on the activity of the catalyst, expressed in the experimental yields [14–17,59], as shown in **Table 1**. To address such differences, we have calculated the activation energy for the overall ROM of the norbornene, that corresponds to the $\Delta\Delta G^{\ddagger}$ of the transition state **bii.12$^{\#}$** regarding the hexacoordinated complex **a**, for each complex with different N^{III} substituent. These results are also reported in **Table 1**.

The values in **Table 1** shows an interesting inverse relation between experimental yields and the activation energy, which is exhibited in **graphic I**, at the bottom part. As it can be seen, the less favorable case is that where the pyridine ligand has a methyl substituent in *para* position (**4-pic**), that is slightly less effective than

Table 1
Comparison of different experimental yields to the activation energy for the overall initiation step and relative stability of the products. The bottom part shows the linear correlation of the experimental yield with the $\Delta\Delta G^{\ddagger}$ for initiation (I) and with products relative stability (II).

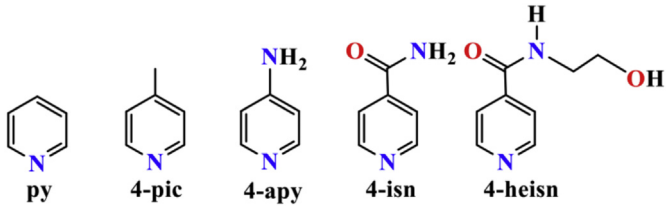

N^{III}[a]	exp. yield (%)[b]	$\Delta\Delta G^{\ddagger}$ for initiation (kcal·mol^{-1})[c]	products (kcal·mol^{-1})[d]
py	43	24.5	−8.9
pic	40	25.0	−7.9
apy	63	14.4	−18.7
isn	94	8.5	−21.8
heisn	94	4.9	−17.1

Fx2

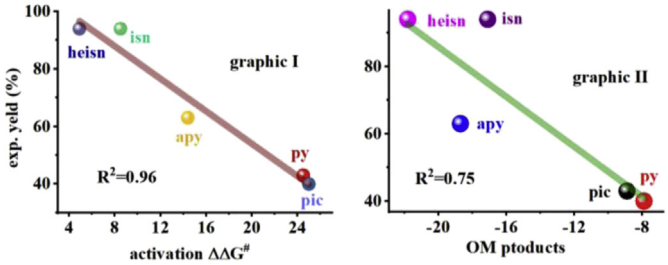

[a] Amine ligand.
[b] polymerization performed at 50 °C/5min, with an initial ratio of [Ru]/[EDA]/[NBE] = 1/5/5000.
[c] Activation initiation energy corresponding to transition state **bii.12**$^{\#}$, regarding the hexacoordinated complex **a**.
[d] Products for the ROM of the norbornene, regarding the hexacoordinated complex.

the pyridine (**py**) itself. This is so because methyl is an electron donating group, which increases the electron density over the metallic center, making the formation of the Ru-carbene double bond (**bii.12**$^{\#}$) harder than in the case of the pyridine. Likewise, the coordination of the olefin in the cycloaddition step (**r.34**$^{\#}$) is more difficult than in the case of the pyridine. In this same sense, the most effective catalysts are the ones with good electron withdrawing groups (**4-isn** and **4-heisn**) because they diminish the electron density over the metallic center. Regarding the relative stability of the ROM products, we found them to have a direct relationship with the experimental yield, depicted in the **graphic II**. This accordance of these experimental results with the critical points of the mechanism is an indicative to the reliability of our model.

4. Concluding remarks

In this contribution, we addressed the formation of the active species ruthenium-carbene, from the complex $[RuCl_2(PPh_3)_2(Py)_2]$ with EDA, and subsequent ROM of norbornene. This complex is an hexacoordinated structure with the similar ligands *trans*-positioned regarding each other.

For the ruthenium-carbene formation we have considered three pathways: **pathway bi**-'diazo linked' is a complex mechanism where the fragment N_2 of EDA is most of the time interacting with the ruthenium atom, with the activation energy of around 52 kcal·mol^{-1}. On the other hand, **pathway bii** - 'direct attack' is more straightforward, where the C_α of EDA interacts with the ruthenium immediatly; this path has an activation energy of around 10 kcal·mol^{-1}, being the most favorable for the formation of the carbene active species $[RuCl_2(Py)_2(=CHCOOEt)]$.

The active carbene species is a 16-electrons species, that releases another pyridine ligand and then the ROM occurs according to the established mechanism for olefin metathesis. In the **pathway c** – 'NBE linked', unlike the others, the norbornene interacts with ruthenium atom before the formation of the ruthenium-carbene, however, with an activation energy of around 26 kcal·mol^{-1}, it is not a reliable alternative.

When analyzed different amine substituent in the initial hexacoordinated complex, the activation energy of the overall catalytic cycle increases and the relative products' energy decreases as the experimental yield decreases, corroborating the reliability of our model.

Conflicts of interest

The authors declare no competing financial interest

Acknowledgment

We would like to thank the brazilian funding agency Coordenação de Aperfeiçoamento de Pessoal de Nível Superior (CAPES) for the research grants of H. G. Evangelista and to Dr. Humberto Soares of Department of Mathematics for computational support.

Supplementary Data

Supplementary data to this article can be found online at https://doi.org/10.1016/j.jorganchem.2019.04.029.

References

[1] D. Astruc, New J. Chem. 29 (2005) 42–56.
[2] R.R. Schrock, Angew. Chem. Int. Ed. 45 (2006) 3748–3759.
[3] Y. Chauvin, Angew. Chem. Int. Ed. 45 (2006) 3741–3747.

[4] R.H. Grubbs, Adv. Synth. Catal. 349 (2007) 34–40.
[5] J.M.E. Matos, N.C. Batista, R.M. Carvalho, S.A.A. Santana, P.N. Puzzi, M. Sanches, B.S. Lima-Neto, Quim. Nova 30 (2007) 431–435.
[6] J.C.M.K.J. Ivin, Olefin Metathesis and Metathesis Polymerization, Academic Press, San Diego, 1997.
[7] J.C. Mol, J. Mol. Catal. A Chem. 213 (2004) 39–45.
[8] P. Jean-Louis Herisson, Y. Chauvin, Makromol. Chem. 141 (1971) 161–176.
[9] R.R. Schrock, Chem. Rev. 109 (2009) 3211–3226.
[10] R.R. Schrock, Chem. Rev. 102 (2002) 145–179.
[11] G.C. Vougioukalakis, R.H. Grubbs 1110 (2010) 1746–1787.
[12] J.A. Love, M.S. Sanford, M.W. Day, R.H. Grubbs, J. Am. Chem. Soc. 125 (2003) 10103–10109.
[13] T.L. Brown, K.J. Lee, Coord. Chem. Rev. 128 (1993) 89–116.
[14] J.M.E. Matos, B.S. Lima-Neto, J. Mol. Catal. A Chem. 222 (2004) 81–85.
[15] J.M.E. Matos, B.S. Lima-Neto, J. Mol. Catal. A Chem. 240 (2005) 233–238.
[16] J.M.E. Matos, B.S. Lima-Neto, Catal. Today 107–108 (2005) 282–288.
[17] J.M.E. Matos, B.S. Lima-Neto, J. Mol. Catal. A Chem. 259 (2006) 286–291.
[18] J.L. Silva Sá, B.S. Lima-Neto, J. Mol. Catal. A Chem. 304 (2009) 187–190.
[19] J.L. Silva Sá, L.H. Vieira, E.S.P. Nascimento, B.S. Lima-Neto, Appl. Catal. Gen. 374 (2010) 194–200.
[20] V.P. Carvalho, C.P. Ferraz, B.S. Lima-Neto, J. Mol. Catal. A Chem. 333 (2010) 46–53.
[21] J.L. Silva Sá, E.S.P. Nascimento, L.R. Fonseca, B.S. Lima-Neto, J. Appl. Polym. Sci. 127 (2013) 3578–3585.
[22] H.K. Chaves, C.P. Ferraz, V.P. Carvalho, B.S. Lima-Neto, J. Mol. Catal. A Chem. 385 (2014) 46–53.
[23] T.B. Silva, R.S. Camargo, B.S. Lima-Neto, J. Braz. Chem. Soc. 25 (2014) 2425–2432.
[24] L.R. Fonseca, J.L. Silva Sá, V.P. Carvalho, B.S. Lima-Neto, Polym. Bull. 75 (2018) 3705–3721.
[25] R.J. Fernandes, T.B. Silva, B.S. Lima-Neto, R.L.A. Haiduke, J. Mol. Catal. A Chem. 410 (2015) 58–65.
[26] A.D. Becke, Phys. Rev. 38 (1988) 3098–3100.
[27] C. Lee, W. Yang, R.G. Parr, Phys. Rev. B 37 (1988) 785–789.
[28] P.C. Hariharan, J.A. Pople, Theor. Chim. Acta 28 (1973) 213–222.
[29] M.M. Francl, W.J. Pietro, W.J. Hehre, J.S. Binkley, M.S. Gordon, D.J. DeFrees, J.A. Pople, J. Chem. Phys. 77 (1982) 3654–3665.
[30] P.J. Hay, W.R. Wadt, J. Chem. Phys. 82 (1985) 299–310.
[31] P.J. Hay, W.R. Wadt, Chem. Phys. 82 (1985) 270–283.
[32] W.R. Wadt, P.J. Hay, J. Chem. Phys. 82 (1985) 284–298.
[33] Y. Zhao, D.G. Truhlar, Theor. Chem. Acc. 120 (2008) 215–241.
[34] R. Krishnan, J.S. Binkley, R. Seeger, J.A. Pople, J. Chem. Phys. 72 (1980) 650–654.
[35] M. Cossi, V. Barone, R. Cammi, J. Tomasi, Chem. Phys. Lett. 255 (1996) 327–335.
[36] V. Barone, M. Cossi, J. Tomasi, J. Chem. Phys. 107 (1997) 3210–3221.
[37] J. Tomasi, B. Mennucci, R. Cammi, Chem. Rev. 105 (2005) 2999–3093.
[38] S. Grimme, J. Antony, S. Ehrlich, H. Krieg, J. Chem. Phys. 132 (2010) 154104.
[39] M.J. Frisch, G.W. Trucks, H.B. Schlegel, G.E. Scuseria, M.A. Robb, J.R. Cheeseman, G. Scalmani, H.B. Barone, B. Mennucci, G.A. Petersson, H. Nakatsuji, M. Caricato, X. Li, M.P. Hratchian, A.F. Izmaylov, J. Bloino, G. Zheng, J.L. Sonnenberg, M. Hada, M. Ehara, K. Toyota, R. Fukuda, J. Hasegawa, J.T. Ishida, T. Nakajima, Y. Honda, O. Kitao, H. Nakai, T. Vreven, J.A. Montgomery, J.E. Peralta, F. Ogliaro, M. Bearpark, J.J. Heyd, E. Brothers, K.N. Kudin, V.N. Staroverov, R. Kobayashi, J. Normand, K. Raghavachari, A. Rendell, J.C. Burant, S.S. Iyengar, J. Tomasi, M. Cossi, N. Rega, J.M. Millam, M. Klene, J.E. Knox, J.B. Cross, V. Bakken, C. Adamo, J. Jaramillo, R. Gomperts, R.E. Stratmann, R.L. Yazyev, A.J. Austin, R. Cammi, C. Pomelli, J.W. Ochterski, R.L. Martin, K. Morokuma, V.G. Zakrzewski, G.A. Voth, P. Salvador, J.J. Dannenberg, S. Dapprich, A.D. Daniels, O. Farkas, J.B. Foresman, J.V. Ortiz, J. Cioslowski, D.J. Fox, Gaussian 09, Revision D.01, Gaussian Inc., Wallingford CT, 2013.
[40] Y.H. Lam, K.N. Houk, J. Am. Chem. Soc. 137 (2015) 2116–2127.
[41] B.K. Mai, K.J. Szabó, F. Himo, ACS Catal. 8 (2018) 4483–4492.
[42] P.H.-Y. Cheong, C.Y. Legault, J.M. Um, N. Çelebi-Ölçüm, K.N. Houk, Chem. Rev. 111 (2011) 5042–5137.
[43] É. De Brito Sá, J.M.E. De Matos, Inorg. Chim. Acta 426 (2015) 20–28.
[44] F. Nuñez-Zarur, X. Solans-Monfort, L. Rodríguez-Santiago, R. Pleixats, M. Sodupe, Chem. Eur J. 17 (2011) 7506–7520.
[45] D. Benitez, E. Tkatchouk, W.A. Goddard, Chem. Commun. (2008) 6194–6196.
[46] L. Simón, J.M. Goodman, Org. Biomol. Chem. 9 (2011) 689–700.
[47] Y.F. Yang, K.N. Houk, Y.D. Wu, J. Am. Chem. Soc. 138 (2016) 6861–6868.
[48] M.N. Grayson, M.J. Krische, K.N. Houk, J. Am. Chem. Soc. 137 (2015) 8838–8850.
[49] X. Hong, D.A. Bercovici, Z. Yang, N. Al-Bataineh, R. Srinivasan, R.C. Dhakal, K.N. Houk, M. J. Am. Chem. Soc. 137 (2015) 9100–9107.
[50] X. Hong, M.C. Stevens, P. Liu, P.A. Wender, K.N. Houk, J. Am. Chem. Soc. 136 (2014) 17273–17283.
[51] B. Kótai, G. Kardos, A. Hamza, V. Farkas, I. Pápai, T. Soós, Chem. Eur J. 20 (2014) 5631–5639.
[52] R. Jagadeesan, G. Sabapathi, J. Madhavan, P. Venuvanalingam, Inorg. Chem. 57 (2018) 6833–6846.
[53] X. Deng, Y. Dang, Z.X. Wang, X. Wang, Organometallics 35 (2016) 1923–1930.
[54] M. Anand, R.B. Sunoj, H.F. Schaefer, ACS Catal. 6 (2016) 696–708.
[55] R. Cohen, B. Rybtchinski, M. Gandelman, H. Rozenberg, J.M.L. Martin, D. J. Am. Chem. Soc. 125 (2003) 6532–6546.
[56] É. De Brito Sá, L. Rodríguez-Santiago, M. Sodupe, X. Solans-Monfort, Organometallics 35 (2016) 3914–3923.
[57] É. De Brito Sá, L. Rodríguez-Santiago, M. Sodupe, X. Solans-Monfort, Organometallics 37 (2018) 1229–1241.
[58] E. De Brito Sá, A. Rimola, L. Rodríguez-Santiago, M. Sodupe, X. Solans-Monfort, J. Phys. Chem. A 122 (2018) 1702–1712.
[59] J.M.E. Matos, Influência de ligantes aminas na reatividade de complexos do tipo $[RuCl_2(PPh_3)_2(amine)_x]$ em reações de metátese de olefinas, Ph. D. Thesis, Universidade de São Paulo, 2005.